Structural Engineering and Mechanics, Vol. 28, No. 2 (2008) 167-188
DOI: http://dx.doi.org/10.12989/sem.2008.28.2.167

On the consideration of the masses of helical springs in damped combined systems consisting of two continua

M. Gürgöze†, S. Zeren‡ and M. M. A. Bicak‡†

Faculty of Mechanical Engineering, Technical University of Istanbul, 34439, Gümüşsuyu, Istanbul, Turkey

(Received September 13, 2006, Accepted September 18, 2007)

Abstract. This study is concerned with the establishment of the characteristic equation of a combined system consisting of a cantilever beam with a tip mass and an in-span visco-elastic helical spring-mass, considering the mass of the helical spring. After obtaining the "exact" characteristic equation of the combined system, by making use of a boundary value problem formulation, the characteristic equation is established via a transfer matrix method, as well. Further, the characteristic equation of a reduced system is obtained as a special case. Then, the characteristic equations are numerically solved for various combinations of the physical parameters. Further, comparison of the results with the massless spring case and the case in which the spring mass is partially considered, reveals the fact that neglecting or considering the mass of the spring partially can cause considerable errors for some combinations of the physical parameters of the system.

Keywords: combined systems; axial vibrations; bending vibrations; visco-elastic continuum; spring-mass attachment; effect of spring mass; free vibrations.

1. Introduction

In the technical literature, many vibrational systems are modelled as Bernoulli-Euler beams to which are attached an arbitray number of spring-mass systems. Gürgöze (1996a) has calculated eigenfrequencies of a clamped-free Bernoulli-Euler beam with a tip mass and a spring-mass system using the Lagrange's multipliers method. Gürgöze (1996b) has also investigated the eigencharacteristics of a beam with a tip mass and a spring-mass system in-span. Qiao *et al.* (2002) have established an exact method for the analysis of free flexural vibrations of non-uniform multi-step Bernoulli-Euler beams carrying an arbitrary number of single-degree-of-freedom and two-degree-of-freedom spring–mass systems. Wu (2002) has conducted a study on determination of the eigenfrequencies and mode shapes of beams carrying any number of two-degree of freedom spring-mass systems by means of two finite element methods. Further, Chen and Wu (2002) have

† Professor, E-mail: gurgozem@itu.edu.tr
‡ MS.c., Research Assistant, E-mail: zerens@gmail.com
‡† MS.c., Research Assistant, E-mail: bicakme@gmail.com

investigated a system consisting of non-uniform beams with multiple spring-mass systems. Some of other recent publications on the subject of Bernoulli-Euler beams to which are attached several one or two-degree of freedom spring-mass-(damper) systems can be cited as Wu and Chou (1999), Wu and Chen (2000), Cha (2001), Wu (2004), and Gökdağ and Kopmaz (2004).

The common aspect of all the above publications is that the mass of the helical springs of the spring-mass systems attached is not taken into account. Although Rayleigh (1945) has revealed that the mass of a linear spring can be taken into account approximately if one third of the spring mass is added to the mass at the end of the spring, it has been observed that the degree of the effects of the massless spring assumption on the numerical values of the eigenfrequencies, in more complicated-combined systems, had not been investigated in the literature.

In the work of Gürgöze (2005), the frequency equation of a classical combined system is derived consisting of a cantilevered beam to the tip of which is attached a helical spring-mass system, the novelty being that the helical spring is modeled as a longitudinally vibrating elastic rod (James *et al.* 1994). The frequency equation obtained is solved numerically for various non-dimensional mass and spring parameters. Comparison with massless spring case reveals that neglecting the mass can lead to serious errors for some parameter combinations. Wu (2005) has taken into account the inertia effects of the helical springs i.e., the masses of the springs, for free vibrations analyses of a Bernoulli-Euler beam carrying multiple two degree-of freedom systems by using equivalent mass method. In a further study, the work of Wu (2006) considered the mass of the helical spring of an absorber system by lumping the corresponding distributed mass of the spring on to the main mass and absorber mass based on finite element considerations. Gürgöze *et al.* (2006) deals with the determination of the frequency equation of a Bernoulli-Euler beam simply supported at both ends, to which is attached in-span a longitudinally vibrating elastic rod with a tip mass, representing a helical spring-mass system with mass of the helical spring considered. Although, essentially, a mechanical system similar to that in the study of Gürgöze (2005) is dealt with here, the present work is an extension of the previous publications Gürgöze (2005) and Gürgöze *et al.* (2006) in that here the boundary conditions are different and more importantly, it is assumed that the helical spring is made of a visco-elastic material (Kelvin-Voigt model). Gürgöze and Zeren (2006) have given the representation of this subsystem, i.e., axially vibrating visco-elastic rod with a tip mass, by a single-degree of freedom spring-damper-mass system.

The principal aim of the present study is the investigation of the effects of not or partially taking into account the mass of the helical spring for some parameter combinations onto the characteristic values. Another aim that the above investigations lead to is to supply the design engineers working in this area with "exact" characteristic equation of the combined system under investigation which can be thought of, for example, as a simple model of an engine or machine tool elastically mounted on a structural element. Further, the characteristic equation of the reduced system is established in which the free end of the longitudinally vibrating rod is fixed. Characteristic equations obtained are solved for various non-dimensional damping, mass and spring parameters and the results are compared with the massless spring case, as well as with the case in which one third of the own mass of the helical spring is added to its end. The "errors" are given, to a great extent, in graphs. It is seen that not taking or taking partially into account the mass of the helical spring can lead to considerable errors for some combinations of the system parameters.

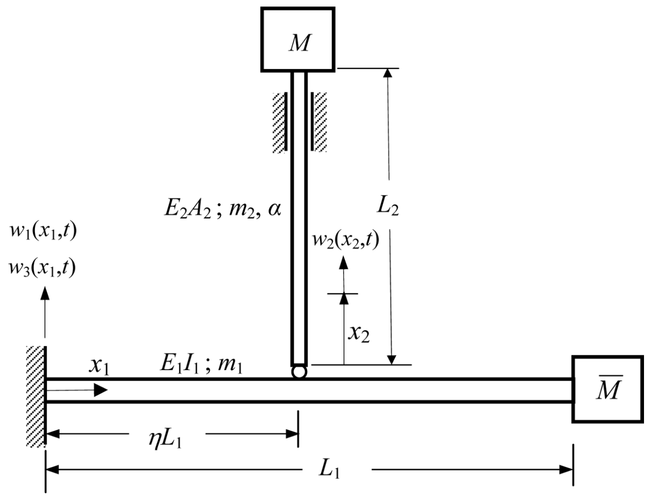

Fig. 1 Vibrational system under study: A cantilevered beam with a tip mass and in-span an axially vibrating visco-elastic rod with a tip mass

2. Theory

2.1 Derivation of the characteristic equation of the system in Fig. 1

The problem to be investigated in the present work is the natural vibration problem of the mechanical system shown in Fig. 1. It consists of a cantilevered Bernoulli-Euler beam with a tip mass to which an axially vibrating visco-elastic rod with tip mass M is attached in-span. Axially vibrating visco-elastic rod with tip mass corresponds to a conventional helical spring-mass system, where the spring is subjected to internal damping. It is assumed that the features of the visco-elastic rod fit the Kelvin-Voigt model and further, that the combined system vibrates only in the plane of the paper. The physical properties of the system are as follows: The length, mass per unit length and bending stiffness of the beam are L_1, m_1, E_1I_1 whereas the corresponding quantities and the axial rigidity of the rod are L_2, m_2, E_2A_2, respectively. $\overline{M}$ denotes the mass of the tip mass on the beam. It is to be noted that E_2A_2/L_2 corresponds to the spring constant of the helical spring and α represents its visco-elastic constant.

The planar bending displacements in the regions to the left and right of the in-span attachment of the visco-elastic rod with tip mass M are denoted as $w_1(x_1, t)$ and $w_3(x_1, t)$ respectively, whereas, the axial displacements of the visco-elastic rod are denoted as $w_2(x_2, t)$ where $x_2 = 0$ corresponds to the attachment point of the rod to the beam. $w_2(x_2, t)$ is actually a "relative" displacement of the rod, with the matching condition $w_2(0,t) = 0$. $w_1(x_1, t)$, $w_2(x_2, t)$ and $w_3(x_1, t)$ are assumed to be small.

In order to obtain the equations of motion of the system, the extended Hamilton's principle

$$\int_{t_0}^{t_1} [\delta(T-V) + \delta' A]\mathrm{d}t = 0 \tag{1}$$

will be applied, where T and V denote the kinetic and potential energies of the system respectively, and $\delta' A$ represents the virtual work of the non-conservative active forces, i.e., here, the damping forces. Although the expressions of T and V could be taken over to some extent from the study of Gürgöze *et al.* (2006), they are given here, for the sake of completeness. The total kinetic energy

$$T = T_1 + T_2 + T_3 + T_4 + T_5 \tag{2}$$

consists of the following parts

$$T_1 = \frac{1}{2} m_1 \int_0^{\eta L_1} \dot{w}_1^2(x_1,t)\mathrm{d}x_1, \quad T_2 = \frac{1}{2} m_2 \int_0^{L_2} [\dot{w}_2(x_2,t) + \dot{w}_1(\eta L_1,t)]^2 \mathrm{d}x_2 \tag{3-4}$$

$$T_3 = \frac{1}{2} m_1 \int_{\eta L_1}^{L_1} \dot{w}_3^2(x_1,t)\mathrm{d}x_1, \quad T_4 = \frac{1}{2} M[\dot{w}_1(\eta L_1,t) + \dot{w}_2(L_2,t)]^2, \quad T_5 = \frac{1}{2}\overline{M}\dot{w}_3^2(L_1,t) \tag{5-7}$$

where the meanings are evident.

The potential energy consists of three parts two of bending and the other due to axial displacements

$$V = V_1 + V_2 + V_3 \tag{8}$$

where

$$V_1 = \frac{1}{2} E_1 I_1 \int_0^{\eta L_1} w_1''^2(x_1,t)\mathrm{d}x_1, \quad V_2 = \frac{1}{2} E_2 A_2 \int_0^{L_2} w_2'^2(x_2,t)\mathrm{d}x_2, \quad V_3 = \frac{1}{2} E_1 I_1 \int_{\eta L_1}^{L_1} w_3''^2(x_1,t)\mathrm{d}x_1 \tag{9-11}$$

In the above formulations, dots and primes denote partial derivatives with respect to time t and the position co-ordinate x_1 or x_2, respectively.

The strain in the visco-elastic rod can be written as

$$\varepsilon = \frac{\partial w_2(x_2,t)}{\partial x_2} := w_2'(x_2,t) \tag{12}$$

Hence, the stress at the section x_2 of the rod associated with the internal damping can be formulated as

$$\sigma_{\mathrm{damp}} = \alpha\dot{\varepsilon} = \alpha w_2'^{\cdot}(x_2,t) \tag{13}$$

Now, $\delta' A$ in Eq. (1) can be formulated in the form

$$\delta' A = \int_0^{L_2} \sigma_{\mathrm{damp}} \delta\varepsilon (A_2 \mathrm{d}x_2) = \int_0^{L_2} (\alpha w_2'^{\cdot}(x_2,t))\,\delta(w_2'(x_2,t)) A_2 \mathrm{d}x_2 \tag{14}$$

which can be found for example in Tauchert (1974), in a general form.

After putting expressions (2) to (11) and (14) into Eq. (1) and carrying out the necessary variations, the following equations of motion of the two beam portions and the visco-elastic rod are obtained

$$E_1 I_1 w_1^{IV}(x_1,t) + m_1 \ddot{w}_1(x_1,t) = 0 \tag{15}$$

$$E_2 A_2 w_2''(x_2,t) + \alpha A_2 \dot{w}_2''(x_2,t) - m_2 \ddot{w}_2(x_2,t) = m_2 \ddot{w}_1(\eta L_1,t) \tag{16}$$

$$E_1 I_1 w_3^{IV}(x_1,t) + m_1 \ddot{w}_3(x_1,t) = 0 \tag{17}$$

The corresponding boundary and matching conditions are as follows

$$w_1(0,t) = 0, \quad w_1'(0,t) = 0, \quad w_2(0,t) = 0, \quad w_3''(L_1,t) = 0 \tag{18-21}$$

$$\overline{M} \ddot{w}_3(L_1,t) - E_1 I_1 w_3'''(L_1,t) = 0 \tag{22}$$

$$w_1(\eta L_1,t) = w_3(\eta L_1,t), \quad w_1'(\eta L_1,t) = w_3'(\eta L_1,t), \quad w_1''(\eta L_1,t) = w_3''(\eta L_1,t) \tag{23-25}$$

$$\int_0^{L_2} m_2[\ddot{w}_2(x_2,t) + \ddot{w}_1(\eta L_1,t)]\mathrm{d}x_2 + M[\ddot{w}_1(\eta L_1,t) + \ddot{w}_2(L_2,t)] - E_1 I_1[w_1'''(\eta L_1,t) - w_3'''(\eta L_1,t)] = 0 \tag{26}$$

$$M[\ddot{w}_1(\eta L_1,t) + \ddot{w}_2(L_2,t)] + E_2 A_2 w_2'(L_2,t) + \alpha A_2 \dot{w}_2'(L_2,t) = 0 \tag{27}$$

One assumes the solutions of the partial differential Eq. (15) to Eq. (17) to be of the form

$$\begin{aligned} w_1(x_1,t) &= W_1(x_1)\mathrm{e}^{\lambda t} \\ w_2(x_2,t) &= W_2(x_2)\mathrm{e}^{\lambda t} \\ w_3(x_1,t) &= W_3(x_1)\mathrm{e}^{\lambda t} \end{aligned} \tag{28}$$

where λ denotes the unknown characteristic value (eigenvalue) of the system which is a complex number in general. In the expressions above, both the displacements w_1, w_2, w_3 and amplitudes W_1, W_2 and W_3 represent complex-valued functions. The essential point here is to imagine the actual displacements w_1, w_2 and w_3 as the real parts of some complex valued functions, for which the same notation is used.

By putting the expressions (28) into the partial differential Eqs. (15)-(17), the following ordinary differential equations for the complex-valued amplitude functions $W_1(x_1), W_2(x_2)$ and $W_3(x_1)$ are obtained

$$W_1^{IV}(x_1) - \beta_b^4 W_1(x_1) = 0 \tag{29}$$

$$W_2''(x_2) - \beta_r^2 W_2(x_2) = \beta_r^2 W_1(\eta L_1) \tag{30}$$

$$W_3^{IV}(x_1) - \beta_b^4 W_3(x_1) = 0 \tag{31}$$

Here, the following abbreviations are introduced

$$\beta_b^4 = -\frac{m_1 \lambda^2}{E_1 I_1}, \quad \beta_r^2 = \frac{m_2 \lambda^2}{E_2 A_2 + \alpha A_2 \lambda} \tag{32}$$

Now, the corresponding boundary and matching conditions are

$$W_1(0) = 0, \quad W_1'(0) = 0, \quad W_2(0) = 0, \quad W_3''(L_1) = 0$$

$$\overline{M}\lambda^2 W_3(L_1) - E_1 I_1 W_3'''(L_1) = 0 \tag{33-37}$$

$$W_1(\eta L_1) = W_3(\eta L_1), \quad W_1'(\eta L_1) = W_3'(\eta L_1), \quad W_1''(\eta L_1) = W_3''(\eta L_1) \tag{38-40}$$

$$\int_0^{L_2} m_2\lambda^2[W_2(x_2) + W_1(\eta L_1)]\mathrm{d}x_2 + M\lambda^2[W_1(\eta L_1) + W_2(L_2)] - E_1 I_1[W_1'''(\eta L_1) - W_3'''(\eta L_1)] = 0 \tag{41}$$

$$M\lambda^2[W_1(\eta L_1) + W_2(L_2)] + E_2 A_2 W_2'(L_2) + \alpha A_2 \lambda W_2'(L_2) = 0 \tag{42}$$

Here, primes over W_i denote derivatives with respect to the corresponding position coordinate x_1 or x_2.

The general solutions of the ordinary differential Eqs. (29)-(31) are

$$W_1(x_1) = C_1 \mathrm{e}^{\beta_b x_1} + C_2 \mathrm{e}^{-\beta_b x_1} + C_3 \mathrm{e}^{\mathrm{i}\beta_b x_1} + C_4 \mathrm{e}^{-\mathrm{i}\beta_b x_1} \tag{43}$$

$$W_3(x_1) = C_5 \mathrm{e}^{\beta_b x_1} + C_6 \mathrm{e}^{-\beta_b x_1} + C_7 \mathrm{e}^{\mathrm{i}\beta_b x_1} + C_8 \mathrm{e}^{-\mathrm{i}\beta_b x_1} \tag{44}$$

$$W_2(x_2) = C_9 \mathrm{e}^{\beta_r x_2} + C_{10} \mathrm{e}^{-\beta_r x_2} - W_1(\eta L_1) \tag{45}$$

where C_1-C_{10} represent ten integration constants yet to be determined and $i = \sqrt{-1}$. Substitution of the expressions in Eqs. (43)-(45) into boundary and matching conditions (33)-(42) yields a set of linear, homogeneous equations consisting of ten equations for the determination of these constants. A non-trivial solution of this set is possible if the determinant of the coefficients equals to zero. After some simple column operations on the determinant, the characteristic equation can be brought into the following form

$$\left| \begin{array}{ccccc}
e^{-\eta\bar{\beta}} & e^{\eta\bar{\beta}} & e^{-\mathrm{i}\eta\bar{\beta}} & e^{\mathrm{i}\eta\bar{\beta}} & 0 \\
e^{-\eta\bar{\beta}} & -e^{\eta\bar{\beta}} & \mathrm{i}e^{-\mathrm{i}\eta\bar{\beta}} & -\mathrm{i}e^{\mathrm{i}\eta\bar{\beta}} & 0 \\
1 & 1 & 1 & 1 & 0 \\
1 & 1 & 1 & 1 & -1 \\
1 & -1 & \mathrm{i} & -\mathrm{i} & -1 \\
1 & 1 & -1 & -1 & -1 \\
-\alpha_{22} & \alpha_{22} & \mathrm{i}\alpha_{22} & -\mathrm{i}\alpha_{22} & \alpha_{22} \\
0 & 0 & 0 & 0 & 0 \\
0 & 0 & 0 & 0 & e^{(1-\eta)\bar{\beta}} \\
0 & 0 & 0 & 0 & (1-\alpha_{44})e^{(1-\eta)\bar{\beta}}
\end{array} \right.$$

$$
\left.\begin{array}{ccccc}
0 & 0 & 0 & 0 & 0 \\
0 & 0 & 0 & 0 & 0 \\
0 & 0 & 0 & -\mathrm{e}^{-\beta_r L_2} & -\mathrm{e}^{\beta_r L_2} \\
-1 & -1 & -1 & 0 & 0 \\
1 & -\mathrm{i} & \mathrm{i} & 0 & 0 \\
-1 & 1 & 1 & 0 & 0 \\
-\alpha_{22} & -\mathrm{i}\alpha_{22} & \mathrm{i}\alpha_{22} & \alpha_{11}+1-\mathrm{e}^{-\beta_r L_2} & \alpha_{11}-1+\mathrm{e}^{\beta_r L_2} \\
0 & 0 & 0 & 1+\alpha_{33}+\alpha_{55}^{*} & 1-\alpha_{33}-\alpha_{55}^{*} \\
\mathrm{e}^{-(1-\eta)\overline{\beta}} & -\mathrm{e}^{\mathrm{i}(1-\eta)\overline{\beta}} & -\mathrm{e}^{-\mathrm{i}(1-\eta)\overline{\beta}} & 0 & 0 \\
(1+\alpha_{44})\mathrm{e}^{-(1-\eta)\overline{\beta}} & (1+\mathrm{i}\alpha_{44})\mathrm{e}^{\mathrm{i}(1-\eta)\overline{\beta}} & (1-\mathrm{i}\alpha_{44})\mathrm{e}^{-\mathrm{i}(1-\eta)\overline{\beta}} & 0 & 0
\end{array}\right| = 0 \qquad (46)
$$

Here, the following non-dimensional parameters are introduced

$$
\overline{\beta} = \beta_b L_1, \quad \alpha_k = \frac{E_2 A_2 / L_2}{E_1 I_1 / L_1^3}, \quad \alpha_M = \frac{M}{m_1 L_1}
$$

$$
\overline{m}_{21} = \frac{m_2 L_2}{m_1 L_1}, \quad \alpha_{\overline{M}} = \frac{\overline{M}}{m_1 L_1}, \quad \overline{d} = \frac{\alpha A_2}{m_1 L_1 L_2 \omega_0}
$$

$$
\omega_0^2 = \frac{E_1 I_1}{m_1 L_1^4}, \quad \beta_r L_2 = \pm \frac{\mathrm{i}\sqrt{\overline{m}_{21}}\,\overline{\beta}^2}{\sqrt{\alpha_k \pm \mathrm{i}\overline{d}\,\overline{\beta}^2}}, \quad \lambda = \pm \mathrm{i}\omega_0 \overline{\beta}^2
$$

$$
\alpha_{11} = \frac{\alpha_M}{\overline{m}_{21}} \beta_r L_2, \quad \alpha_{22} = -\frac{1}{\overline{m}_{21}\overline{\beta}} \beta_r L_2, \quad \alpha_{33} = -\frac{\alpha_k}{\alpha_M \overline{\beta}^4} \beta_r L_2
$$

$$
\alpha_{44} = -\frac{1}{\alpha_{\overline{M}}\overline{\beta}}, \quad \alpha_{55}^{*} = -\frac{\mathrm{i}\overline{d}\beta_r L_2}{\alpha_M \overline{\beta}^2} \qquad (47)
$$

The roots of the characteristic Eq. (46) give us the dimensionless characteristic values $\overline{\beta}$ and therefore by considering Eq. (32), the characteristic values, i.e., eigenvalues -λ- of the system in Fig. 1.

The size of the determinant in the characteristic equation of the system in Fig. 1 in which only one longitudinally vibrating visco-elastic rod with a tip mass (i.e., one spring-damper-mass system) is attached to the bending beam, is 10 × 10, as it is seen from Eq. (46). Any additional visco-elastic rod with a tip mass to be attached to the system would increase the size of the characteristic determinant by 6. Therefore, it is reasonable to expect encountering numerical difficulties in case of a system with several longitudinally vibrating rods with tip masses. Hence, in the following section, an alternative form of the characteristic equation will be derived which essentially is based on the transfer matrix method which has been succesfully applied by Li and his co-authors (2000a, 2000b, 2002) to various vibrational systems. This would first of all, enable one to check the numerical results obtained via the boundary value problem approach, as the corresponding numerical results are not available in the technical literature.

On the other side, the characteristic equation of the system in case of the attachment of additional rod-tip mass systems, could easily be established and then solved numerically with less difficulties, as the attachment of any additional rod-tip mass systems would lead to the multiplication of the actual 4 × 4 overall transfer matrix by an additional 4 × 4 transfer matrix.

2.2 Alternative form of the characteristic equation via the transfer matrix method

As a first step to derive the alternative form, rewriting the amplitude functions for the different portions of the system given in Eqs. (43)-(45) as

$$W_1(\bar{x}_1) = C_1 e^{\bar{\beta}\bar{x}_1} + C_2 e^{-\bar{\beta}\bar{x}_1} + C_3 e^{i\bar{\beta}\bar{x}_1} + C_4 e^{-i\bar{\beta}\bar{x}_1} \tag{48}$$

$$W_3(\bar{x}_1) = C_5 e^{\bar{\beta}\bar{x}_1} + C_6 e^{-\bar{\beta}\bar{x}_1} + C_7 e^{i\bar{\beta}\bar{x}_1} + C_8 e^{-i\bar{\beta}\bar{x}_1} \tag{49}$$

$$W_2(\bar{x}_2) = C_9 e^{\beta_r L_2 \bar{x}_2} + C_{10} e^{-\beta_r L_2 \bar{x}_2} - W_1(\eta) \tag{50}$$

where non-dimensional position coordinates are introduced as

$$\bar{x}_1 = x_1/L_1, \quad \bar{x}_2 = x_2/L_2 \tag{51}$$

The relationship between the parameters W_{10} (bending displacement), W'_{10} (slope), M_{10} (bending moment) and Q_{10} (shear force) at the left end, to W_{11}, W'_{11}, M_{11}, Q_{11} at the right end of the beam region 1 can be expressed in matrix notations as

$$\begin{bmatrix} W_{11} \\ \dfrac{L_1}{\bar{\beta}} W'_{11} \\ \dfrac{L_1^2}{\bar{\beta}^2 k_1} M_{11} \\ \dfrac{L_1^3}{\bar{\beta}^3 k_1} Q_{11} \end{bmatrix} = [\bar{T}_1] \begin{bmatrix} W_{10} \\ \dfrac{L_1}{\bar{\beta}} W'_{10} \\ \dfrac{L_1^2}{\bar{\beta}^2 k_1} M_{10} \\ \dfrac{L_1^3}{\bar{\beta}^3 k_1} Q_{10} \end{bmatrix} \tag{52}$$

where $k_1 = E_1 I_1$ and the transfer matrix $[\bar{T}_1]$ reads as

$$[\bar{T}_1] = \begin{bmatrix} e^{\eta\bar{\beta}} & e^{-\eta\bar{\beta}} & e^{i\eta\bar{\beta}} & e^{-i\eta\bar{\beta}} \\ e^{\eta\bar{\beta}} & -e^{-\eta\bar{\beta}} & ie^{i\eta\bar{\beta}} & -ie^{-i\eta\bar{\beta}} \\ e^{\eta\bar{\beta}} & e^{-\eta\bar{\beta}} & -e^{i\eta\bar{\beta}} & -e^{-i\eta\bar{\beta}} \\ -e^{\eta\bar{\beta}} & e^{-\eta\bar{\beta}} & ie^{i\eta\bar{\beta}} & -ie^{-i\eta\bar{\beta}} \end{bmatrix} \begin{bmatrix} 1 & 1 & 1 & 1 \\ 1 & -1 & i & -i \\ 1 & 1 & -1 & -1 \\ -1 & 1 & i & -i \end{bmatrix}^{-1} \tag{53}$$

It is to be noted that the coefficients of slope, bending moment and shear force assure that the elements of the transfer matrix are dimensionless.

After lengthy calculations, it can be shown that the transfer matrix $[\bar{T}_2]$ relating the parameters to the left of the attachment point of the rod to the beam to those to the right is of the form

$$[\overline{T}_2] = \begin{bmatrix} 1 & 0 & 0 & 0 \\ 0 & 1 & 0 & 0 \\ 0 & 0 & 1 & 0 \\ \overline{A}_{910} & 0 & 0 & 1 \end{bmatrix} \tag{54}$$

where the following abbreviations are introduced

$$\overline{A}_{910} = -\overline{\beta}\left\{\left[\frac{\overline{m}_{21}}{\beta_r L_2}(\mathrm{e}^{\beta_r L_2}-1)+\alpha_M \mathrm{e}^{\beta_r L_2}\right]\alpha_9 + \left[\frac{\overline{m}_{21}}{\beta_r L_2}(1-\mathrm{e}^{-\beta_r L_2})+\alpha_M \mathrm{e}^{-\beta_r L_2}\right]\alpha_{10}\right\}$$

$$\alpha_9 = \frac{(1-\alpha_{33}-\overset{*}{\alpha}_{55})\mathrm{e}^{-\beta_r L_2}}{(1-\alpha_{33}-\overset{*}{\alpha}_{55})\mathrm{e}^{-\beta_r L_2}-(1+\alpha_{33}+\overset{*}{\alpha}_{55})\mathrm{e}^{\beta_r L_2}}$$

$$\alpha_{10} = -\frac{(1+\alpha_{33}+\overset{*}{\alpha}_{55})\mathrm{e}^{\beta_r L_2}}{(1-\alpha_{33}-\overset{*}{\alpha}_{55})\mathrm{e}^{-\beta_r L_2}-(1+\alpha_{33}+\overset{*}{\alpha}_{55})\mathrm{e}^{\beta_r L_2}}$$

$$\alpha_{33} = -\frac{\alpha_k}{\alpha_M \overline{\beta}^4}\beta_r L_2 \tag{55}$$

Further, the transfer matrix $[\overline{T}_3]$ interrelating the parameters at the left end of the beam portion 3 to those at the right end is

$$[\overline{T}_3] = \begin{bmatrix} \mathrm{e}^{\overline{\beta}} & \mathrm{e}^{-\overline{\beta}} & \mathrm{e}^{\mathrm{i}\overline{\beta}} & \mathrm{e}^{-\mathrm{i}\overline{\beta}} \\ \mathrm{e}^{\overline{\beta}} & -\mathrm{e}^{-\overline{\beta}} & \mathrm{i}\mathrm{e}^{\mathrm{i}\overline{\beta}} & -\mathrm{i}\mathrm{e}^{-\mathrm{i}\overline{\beta}} \\ \mathrm{e}^{\overline{\beta}} & \mathrm{e}^{-\overline{\beta}} & -\mathrm{e}^{\mathrm{i}\overline{\beta}} & -\mathrm{e}^{-\mathrm{i}\overline{\beta}} \\ -\mathrm{e}^{\overline{\beta}} & \mathrm{e}^{-\overline{\beta}} & \mathrm{i}\mathrm{e}^{\mathrm{i}\overline{\beta}} & -\mathrm{i}\mathrm{e}^{-\mathrm{i}\overline{\beta}} \end{bmatrix} \begin{bmatrix} \mathrm{e}^{\eta\overline{\beta}} & \mathrm{e}^{-\eta\overline{\beta}} & \mathrm{e}^{\mathrm{i}\eta\overline{\beta}} & \mathrm{e}^{-\mathrm{i}\eta\overline{\beta}} \\ \mathrm{e}^{\eta\overline{\beta}} & -\mathrm{e}^{-\eta\overline{\beta}} & \mathrm{i}\mathrm{e}^{\mathrm{i}\eta\overline{\beta}} & -\mathrm{i}\mathrm{e}^{-\mathrm{i}\eta\overline{\beta}} \\ \mathrm{e}^{\eta\overline{\beta}} & \mathrm{e}^{-\eta\overline{\beta}} & -\mathrm{e}^{\mathrm{i}\eta\overline{\beta}} & -\mathrm{e}^{-\mathrm{i}\eta\overline{\beta}} \\ -\mathrm{e}^{\eta\overline{\beta}} & \mathrm{e}^{-\eta\overline{\beta}} & \mathrm{i}\mathrm{e}^{\mathrm{i}\eta\overline{\beta}} & -\mathrm{i}\mathrm{e}^{-\mathrm{i}\eta\overline{\beta}} \end{bmatrix}^{-1} \tag{56}$$

Finally, the transfer matrix between the parameters at the left and right ends of the tip mass $\overline{M}$ can be shown to be

$$[\overline{T}_{\overline{M}}] = \begin{bmatrix} 1 & 0 & 0 & 0 \\ 0 & 1 & 0 & 0 \\ 0 & 0 & 1 & 0 \\ -\alpha_{\overline{M}}\overline{\beta} & 0 & 0 & 1 \end{bmatrix} \tag{57}$$

Combining the results obtained so far, the overall transfer matrix $[\overline{T}]$ of the vibrational system in Fig. 1, the matrix relating the quantities W_{10}, W'_{10}, M_{10} and Q_{10} at the left end of the system and those at the right end, i.e., $\overline{W}_{31}, \overline{W}'_{31}, \overline{M}_{31}, \overline{Q}_{31}$ can be shown to be

$$[\overline{T}] = [\overline{T}_{\overline{M}}][\overline{T}_3][\overline{T}_2][\overline{T}_1] = \begin{bmatrix} \overline{T}_{11} & \overline{T}_{12} & \overline{T}_{13} & \overline{T}_{14} \\ \overline{T}_{21} & \overline{T}_{22} & \overline{T}_{23} & \overline{T}_{24} \\ \overline{T}_{31} & \overline{T}_{32} & \overline{T}_{33} & \overline{T}_{34} \\ \overline{T}_{41} & \overline{T}_{42} & \overline{T}_{43} & \overline{T}_{44} \end{bmatrix} \tag{58}$$

In the case of the vibrational system in Fig. 1, the boundary conditions are such that the bending displacement and slope at the left end, the bending moment and shear force at the right end of the system vanish: $W_{10} = W'_{10} = \overline{M}_{31} = \overline{Q}_{31} = 0$. These lead to the characteristic equation

$$\begin{vmatrix} \overline{T}_{33} & \overline{T}_{34} \\ \overline{T}_{43} & \overline{T}_{44} \end{vmatrix} = 0 \tag{59}$$

If there is no tip mass on the bending beam, i.e., $\overline{M} = 0$, the matrix $[\overline{T}_{\overline{M}}]$ reduces to the 4×4 unit matrix. Hence, the overall transfer matrix $[\overline{T}]$ reduces to

$$[\overline{T}] = [\overline{T}_3][\overline{T}_2][\overline{T}_1] \tag{60}$$

The characteristic Eq. (59) holds in form where $\overline{T}_{33}, \overline{T}_{34}, \overline{T}_{43}$ and $\overline{T}_{44}$ denote in this case, the corresponding elements of the matrix $[\overline{T}]$ given in Eq. (60).

2.3 Derivation of the characteristic equation of the system in Fig. 2

Unfortunately, it is not possible to obtain the characteristic equation of this system from that in Fig. 1 simply by letting $M \to \infty$ (i.e., $\alpha_M \to \infty$) in the characteristic Eq. (46). It can be shown that in the previous boundary conditions (18)-(27), the conditions (26) and (27) have to be replaced by the following two expressions respectively

$$\int_0^{L_2} m_2[\ddot{w}_2(x_2,t) + \ddot{w}_1(\eta L_1,t)]\mathrm{d}x_2 - E_2A_2w_2'(L_2,t) - E_1I_1[w_1'''(\eta L_1,t) - w_3'''(\eta L_1,t)] - \alpha A_2 w_2'^{\cdot}(L_2,t) = 0 \tag{61}$$

$$w_1(\eta L_1,t) + w_2(L_2,t) = 0 \tag{62}$$

whereas the remaining eight conditions are unchanged.

Exponential solutions of the form Eq. (28) lead for the amplitude functions to

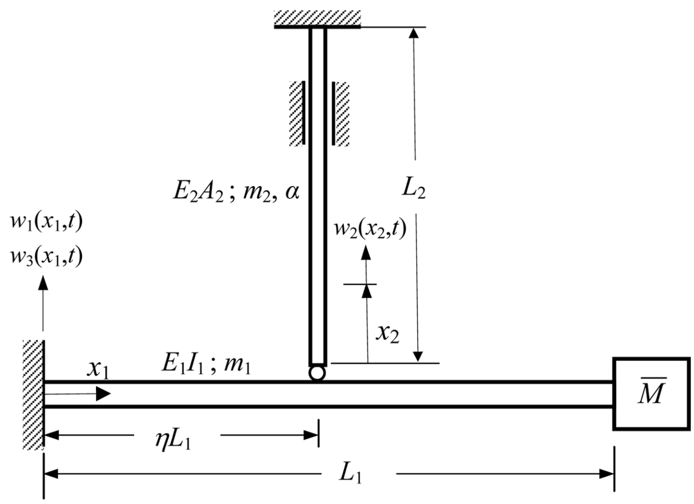

Fig. 2 Vibrational system in Fig. 1 for the limit $M \to \infty$ (i.e., $\alpha_M \to \infty$)

$$\int_0^{L_2} m_2\lambda^2[W_2(x_2)+W_1(\eta L_1)]\mathrm{d}x_2 - E_2A_2W_2'(L_2) - E_1I_1[W_1'''(\eta L_1) - W_3'''(\eta L_1)] - \alpha A_2\lambda W_2'(L_2) = 0 \tag{63}$$

$$W_1(\eta L_1) + W_2(L_2) = 0 \tag{64}$$

which correspond to Eqs. (41) and (42).

Substitution of Eqs. (43)-(45) into the boundary and matching conditions yields a set of ten homogeneous equations for the determination of the ten coefficients C_1-C_{10}. Setting the corresponding determinant of coefficients to zero, and applying some elemantary column operations on the corresponding determinant, results in the following characteristic equation for the vibrational system in Fig. 2

$$\begin{vmatrix}
e^{-\eta\bar\beta} & e^{\eta\bar\beta} & e^{-\mathrm{i}\eta\bar\beta} & e^{\mathrm{i}\eta\bar\beta} & 0 & 0 & 0 & 0 & 0 & 0 \\
e^{-\eta\bar\beta} & -e^{\eta\bar\beta} & \mathrm{i}e^{-\mathrm{i}\eta\bar\beta} & -\mathrm{i}e^{\mathrm{i}\eta\bar\beta} & 0 & 0 & 0 & 0 & 0 & 0 \\
1 & 1 & 1 & 1 & 0 & 0 & 0 & 0 & -\mathrm{e}^{-\beta_r L_2} & -\mathrm{e}^{\beta_r L_2} \\
1 & 1 & 1 & 1 & -1 & -1 & -1 & -1 & 0 & 0 \\
1 & -1 & \mathrm{i} & -\mathrm{i} & -1 & 1 & -\mathrm{i} & \mathrm{i} & 0 & 0 \\
1 & 1 & -1 & -1 & -1 & -1 & 1 & 1 & 0 & 0 \\
-\alpha_{22} & \alpha_{22} & \mathrm{i}\alpha_{22} & -\mathrm{i}\alpha_{22} & \alpha_{22} & -\alpha_{22} & -\mathrm{i}\alpha_{22} & \mathrm{i}\alpha_{22} & 1-\alpha_{55}-\bar\alpha_{55}-\mathrm{e}^{-\beta_r L_2} & \alpha_{55}+\bar\alpha_{55}-1+\mathrm{e}^{\beta_r L_2} \\
0 & 0 & 0 & 0 & 0 & 0 & 0 & 0 & 1 & 1 \\
0 & 0 & 0 & 0 & e^{(1-\eta)\bar\beta} & \mathrm{e}^{-(1-\eta)\bar\beta} & -\mathrm{e}^{\mathrm{i}(1-\eta)\bar\beta} & -\mathrm{e}^{-\mathrm{i}(1-\eta)\bar\beta} & 0 & 0 \\
0 & 0 & 0 & 0 & (1-\alpha_{44})e^{(1-\eta)\bar\beta} & (1+\alpha_{44})\mathrm{e}^{-(1-\eta)\bar\beta} & (1+\mathrm{i}\alpha_{44})\mathrm{e}^{\mathrm{i}(1-\eta)\bar\beta} & (1-\mathrm{i}\alpha_{44})\mathrm{e}^{-\mathrm{i}(1-\eta)\bar\beta} & 0 & 0
\end{vmatrix} = 0 \tag{65}$$

where two additional definitions are introduced as

$$\alpha_{55} = -\frac{\alpha_k(\beta_r L_2)^2}{\bar m_{21}\bar\beta^4}, \quad \bar\alpha_{55} = \frac{\mathrm{i}\bar d\bar\beta^2}{(\alpha_k \pm \mathrm{i}\bar d\bar\beta^2)} \tag{66}$$

Based on the same argumentation as for the system in Fig. 1, in the next section, an alternative formulation of the characteristic equation of the system in Fig. 2 will be given.

2.4 Alternative formulation of the characteristic equation of the system in Fig. 2 via the transfer matrix method.

Fortunately, all transfer matrices in section 2.2 remain the same, except the transfer matrix $[\overline{T}_2]$ which transforms the parameters to the left of the attachment point of the vertical rod to the bending beam, to those to the right. It reads now

$$[\overline{T}_2] = \begin{bmatrix} 1 & 0 & 0 & 0 \\ 0 & 1 & 0 & 0 \\ 0 & 0 & 1 & 0 \\ \overline{\overline{A}}_{910} & 0 & 0 & 1 \end{bmatrix} \tag{67}$$

where, the following abbreviations are introduced

$$\overline{\overline{A}}_{910} = [-\alpha_{66}(e^{\beta_r L_2}-1)-(\alpha_{77}+\alpha_{88})e^{\beta_r L_2}]\overline{\alpha}_9+[(-\alpha_{66}(1-e^{-\beta_r L_2}))+(\alpha_{77}+\alpha_{88})e^{-\beta_r L_2}]\overline{\alpha}_{10}$$

$$\overline{\alpha}_9 = \frac{1}{\Delta}e^{-\beta_r L_2}, \quad \overline{\alpha}_{10} = -\frac{1}{\Delta}e^{\beta_r L_2}, \quad \Delta = e^{-\beta_r L_2}-e^{\beta_r L_2}$$

$$\alpha_{66} = -\frac{\overline{m}_{21}}{\beta_r L_2}\overline{\beta}, \quad \alpha_{77} = \frac{\alpha_k}{\overline{\beta}^3}\beta_r L_2, \quad \alpha_{88} = \frac{\mathrm{i}\overline{d}}{\overline{\beta}}\beta_r L_2 \tag{68}$$

Having obtained the characteristic equation of the vibrational systems in Figs. 1 and 2, it is reasonable to obtain numerical results and make comparisons with those systems which correspond to limit cases of both systems. Recognizing that $\overline{m}_{21}$ denotes the ratio of the mass of the longitudinally vibrating rod to that of the bending beam, it is clear that the limit $\overline{m}_{21} \to 0$ corresponds to the simplified systems in which the visco-elastic rod is discretized by a spring-damper-mass system, in Figs. 3 and 4 for $\overline{\delta}=0, k = E_2A_2/L_2$ and $d = \alpha A_2/L_2$. Unfortunately, it is

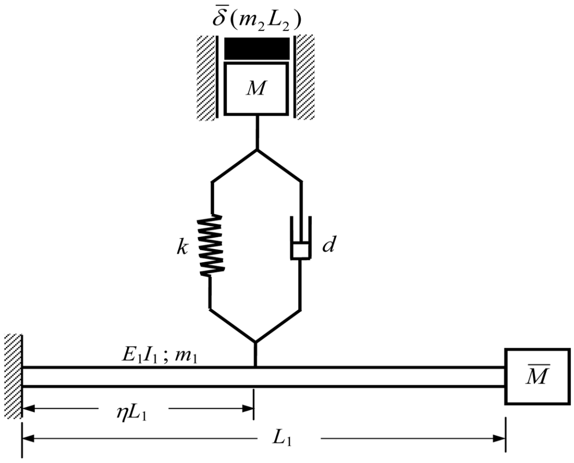

Fig. 3 Simplified representation of the vibrational system in Fig. 1

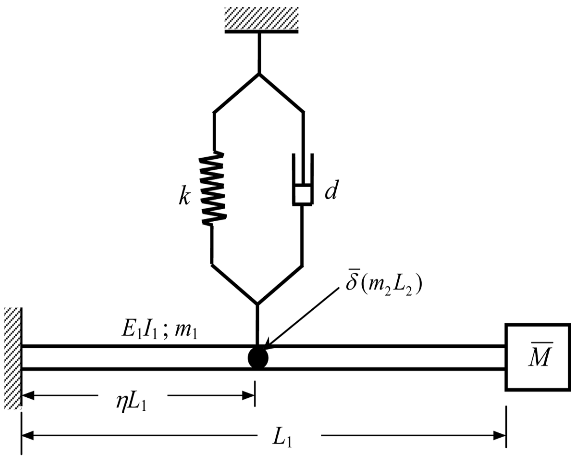

Fig. 4 Simplified representation of the vibrational system in Fig. 2

not possible to obtain their characteristic equations simply by taking the limit $\overline{m}_{21} \rightarrow 0$ in the previous Eqs. (46) and (65), as expected. Hence, the need arises to derive the characteristic equations of these systems. Although the characteristic equations especially of the system in Fig. 3 might be found in the technical literature, for the sake of completeness, characteristic equations of both systems are given in the appendix in the notations of the present study, without any derivation: (A1), (A2).

A look at Figs. 3 and 4 reveals that a point mass $\overline{\delta} m_2 L_2$ is attached to the tip mass M and to the attachment point of the spring-damper to the bending beam, respectively. It is clear that $\overline{\delta}$ represents a factor which indicates to which extent the own mass of the spring is accounted for. $\overline{\delta} = 0$ corresponds to the limit case where the spring mass is fully neglected, i.e., $\overline{m}_{21} \rightarrow 0$. This is the case which is encountered in practice in general. A more realistic application would be that a design engineer adds one third of the spring mass to the mass at the end of the spring, which in turn would mean $\overline{\delta} = 1/3$.

In the next section, numerical values of characteristic values obtained from equations established in the present study, will be compared with those obtained via the simplified systems in Figs. 3 and 4 by taking $\overline{\delta} = 0$ and 1/3, respectively. The comparison of the numerical results obtained will put forward the fact that neglecting or not fully taking into account the distributed mass of the visco-elastic spring can lead, for some combinations of the system parameters, to significant errors in the numerical values of the characteristic values of the actual vibrational system.

3. Numerical results

This section is devoted to the numerical evaluation of the formulas established in the preceding section. Recognizing that $\overline{m}_{21} = 0$ corresponds to the case of the mass of the axially vibrating visco-elastic rod in Fig. 1, i.e., the helical spring, being zero, it is reasonable to make a comparison with the numerical values resulting from the system in Fig. 3 for $\overline{\delta} = 0$.

$\overline{\delta}$ in Fig. 3 represents a non-dimensional factor which indicates to which extent the own mass of the helical spring is accounted for. Further, $\overline{\delta} = 1/3$ corresponds to the case in which one third of the mass of the helical spring is added to the mass at the tip in order to consider the mass of the spring somewhat more realistically.

The characteristic values (in short, the eigenvalues) λ of the system in Fig. 1 are given in Table 1 in the form of λ/ω_0 for various values of the non-dimensional mass and stiffness parameters α_M, $\overline{m}_{21}$ and α_k, where $\overline{d} = 0.1$, $\eta = 0.5$ and $\alpha_{\overline{M}} = 0.5$ are taken. The bold complex numbers in the first sub-cell in each $\alpha_M - \alpha_k$ cell represent the eigenvalues for the massless spring case which corresponds to $\overline{\delta} = 0$, for the assumption: $\overline{m}_{21} \rightarrow 0$. The complex numbers in the second, third and fourth sub-cells represent the eigenvalues for the cases $\overline{m}_{21} = 0.01$, 0.1 and 0.5, respectively. The first number in each of these sub-cells corresponds to the system in Fig. 3 for $\overline{\delta} = 1/3$ and they are obtained from (A1). The second numbers which are indicated by "P" are the values obtained from the numerical solution of the present characteristic Eq. (46) considering the definitions given in Eqs. (32) and (47). The roots of the characteristic Eq. (59) based on the transfer matrix method are also numerically obtained. But they are exactly the same as from Eq. (46), so they are not repeated in Table 1. All numerical calculations were carried out with MATLAB.

Before proceeding further, it is quite instructive to report in the beginning on the experience gained during the solution of the complex Eq. (46) with respect to $\overline{\beta}$. In case of "+" sign in the

Table 1 The characteristic values of the system in Fig. 1 in the form of λ/ω_0 for various values of the stiffness and mass parameter α_k, α_M and $\overline{m}_{21}$

			α_k				
α_M	$\overline{m}_{21}$		0.5	1	2	5	10
0.5	0	$\overline{\delta}=0$	**−0.094476±0.983359i**	**−0.083426±1.366236i**	**−0.035189±1.759166i**	**−0.002039±1.912021i**	**−0.000344±1.933800i**
	0.01	$\overline{\delta}=1/3$	−0.093863±0.980140i	−0.082983±1.361891i	−0.035524±1.755655i	−0.002072±1.911045i	−0.000349±1.933165i
		P	−0.093827±0.980059i	−0.082885±1.361598i	−0.035430±1.754661i	−0.002077±1.910034i	−0.000350±1.932231i
	0.1	$\overline{\delta}=1/3$	−0.088685±0.952522i	−0.079145±1.324520i	−0.038137±1.723809i	−0.002383±1.902076i	−0.000394±1.927406i
		P	−0.088297±0.951431i	−0.078252±1.321407i	−0.037156±1.714291i	−0.002433±1.891927i	−0.000407±1.918086i
	0.5	$\overline{\delta}=1/3$	−0.071201±0.853006i	−0.065160±1.188701i	−0.042441±1.586632i	−0.004022±1.858178i	−0.000629±1.900760i
		P	−0.069290±0.844838i	−0.062020±1.172272i	−0.038222±1.548105i	−0.004177±1.807895i	−0.000702±1.854960i
1	0	$\overline{\delta}=0$	**−0.047664±0.697612i**	**−0.044624±0.974221i**	**−0.035890±1.327209i**	**−0.008660±1.726351i**	**−0.001411±1.827549i**
	0.01	$\overline{\delta}=1/3$	−0.047507±0.696459i	−0.044482±0.972623i	−0.035808±1.325163i	−0.008699±1.724946i	−0.001420±1.826778i
		P	−0.047499±0.696433i	−0.044465±0.972540i	−0.035770±1.324892i	−0.008685±1.724150i	−0.001420±1.825923i
	0.1	$\overline{\delta}=1/3$	−0.046138±0.686339i	−0.043246±0.958587i	−0.035081±1.307143i	−0.009047±1.712281i	−0.001499±1.819810i
		P	−0.046055±0.686019i	−0.043074±0.957706i	−0.034720±1.304441i	−0.008898±1.704469i	−0.001495±1.811341i
	0.5	$\overline{\delta}=1/3$	−0.040898±0.646162i	−0.038480±0.902805i	−0.032046±1.234741i	−0.010330±1.656068i	−0.001859±1.788323i
		P	−0.040437±0.643741i	−0.037693±0.897635i	−0.030608±1.221810i	−0.009513±1.620566i	−0.001809±1.747893i
1.5	0	$\overline{\delta}=0$	**−0.031853±0.570212i**	**−0.030143±0.797141i**	**−0.026016±1.094924i**	**−0.011795±1.523593i**	**−0.002719±1.707653i**
	0.01	$\overline{\delta}=1/3$	−0.031783±0.569582i	−0.029880±0.796755i	−0.025966±1.093751i	−0.011800±1.522357i	−0.002727±1.706843i
		P	−0.031779±0.569568i	−0.030070±0.796222i	−0.025951±1.093622i	−0.011781±1.521868i	−0.002724±1.706133i
	0.1	$\overline{\delta}=1/3$	−0.031164±0.564006i	−0.029502±0.788497i	−0.025522±1.083365i	−0.011838±1.511324i	−0.002797±1.699566i
		P	−0.031129±0.563845i	−0.029433±0.788055i	−0.025379±1.082062i	−0.011655±1.506534i	−0.002761±1.692557i
	0.5	$\overline{\delta}=1/3$	−0.028681±0.541067i	−0.027190±0.756533i	−0.023709±1.040494i	−0.011883±1.464249i	−0.003087±1.667401i
		P	−0.028487±0.539908i	−0.026852±0.753950i	−0.023080±1.033933i	−0.011074±1.442336i	−0.002892±1.634490i
2	0	$\overline{\delta}=0$	**−0.023917±0.494083i**	**−0.022732±0.691015i**	**−0.020092±0.952068i**	**−0.011461±1.360173i**	**−0.003645±1.589401i**
	0.01	$\overline{\delta}=1/3$	−0.023877±0.493673i	−0.022695±0.690443i	−0.020061±0.951294i	−0.011455±1.359225i	−0.003644±1.588084i
		P	−0.023875±0.493664i	−0.022691±0.690417i	−0.020053±0.951215i	−0.011442±1.358914i	−0.003644±1.588084i
	0.1	$\overline{\delta}=1/3$	−0.023526±0.490029i	−0.022365±0.685359i	−0.019788±0.944405i	−0.011395±1.350763i	−0.003688±1.581860i
		P	−0.023507±0.489929i	-0.022328±0.685084i	−0.019713±0.943609i	−0.011268±1.347703i	−0.003635±1.576352i
	0.5	$\overline{\delta}=1/3$	−0.022082±0.474758i	−0.021009±0.664049i	−0.018656±0.915493i	−0.011111±1.314764i	−0.003837±1.552255i
		P	−0.021978±0.474070i	−0.020823±0.662466i	−0.018310±0.911427i	−0.010545±1.300419i	−0.003579±1.526439i

Table 1 Continued

			α_k				
α_M	$\overline{m}_{21}$		0.5	1	2	5	10
2.5	0	$\overline{\delta}$ =0	**−0.019146±0.442063i**	**−0.018241±0.618407i**	**−0.016312±0.853382i**	**−0.010333±1.235035i**	**−0.004072±1.482454i**
	0.01	$\overline{\delta}$ =1/3	−0.019120±0.441769i	−0.018217±0.617997i	−0.016291±0.852823i	−0.010326±1.234303i	−0.004074±1.481788i
		P	−0.019119±0.441763i	−0.018215±0.617978i	−0.016287±0.852769i	−0.010317±1.234089i	−0.004068±1.481353i
	0.1	$\overline{\delta}$ =1/3	−0.018894±0.439152i	−0.018004±0.614343i	−0.016109±0.847841i	−0.010255±1.227778i	−0.004087±1.475818i
		P	−0.018883±0.439083i	−0.017981±0.614151i	−0.016063±0.847292i	−0.010168±1.225654i	−0.004033±1.471523i
	0.5	$\overline{\delta}$ =1/3	−0.017952±0.428060i	−0.017113±0.598851i	−0.015344±0.826703i	−0.009943±1.199903i	−0.004131±1.449897i
		P	−0.017887±0.427598i	−0.016997±0.597764i	−0.015127±0.823886i	−0.009553±1.189775i	−0.003878±1.429659i
3	0	$\overline{\delta}$ =0	**−0.015961±0.403633i**	**−0.015230±0.564729i**	**−0.013714±0.780062i**	**−0.009202±1.137392i**	**−0.004165±1.389391i**
	0.01	$\overline{\delta}$ =1/3	−0.015944±0.403409i	−0.015213±0.564417i	−0.013699±0.779635i	−0.009195±1.136813i	−0.004165±1.388816i
		P	−0.015943±0.403404i	−0.015212±0.564403i	−0.013696±0.779594i	−0.009189±1.136655i	−0.004160±1.388473i
	0.1	$\overline{\delta}$ =1/3	−0.015786±0.401413i	−0.015064±0.561629i	−0.013569±0.775819i	−0.009132±1.131642i	−0.004164±1.383667i
		P	−0.015778±0.401361i	−0.015048±0.561485i	−0.013538±0.775412i	−0.009071±1.130070i	−0.004116±1.380271i
	0.5	$\overline{\delta}$ =1/3	−0.015123±0.392889i	−0.014436±0.549719i	−0.013020±0.759512i	−0.008858±1.109452i	−0.004151±1.361337i
		P	−0.015079±0.392555i	−0.014356±0.548917i	−0.012872±0.757420i	−0.008578±1.101867i	−0.003927±1.345218i
5	0	$\overline{\delta}$ =0	**−0.009585±0.312786i**	**−0.009171±0.437743i**	**−0.008358±0.605708i**	**−0.006140±0.894300i**	**−0.003532±1.127644i**
	0.01	$\overline{\delta}$ =1/3	−0.009578±0.312681i	−0.009165±0.437597i	−0.008352±0.605507i	−0.006136±0.894014i	−0.003531±1.127316i
		P	−0.009578±0.312679i	−0.009164±0.437591i	−0.008351±0.605489i	−0.006134±0.893945i	−0.003528±1.127153i
	0.1	$\overline{\delta}$ =1/3	−0.009521±0.311749i	−0.009111±0.436294i	−0.008304±0.603713i	−0.006104±0.891452i	−0.003519±1.124373i
		P	−0.009519±0.311726i	−0.009105±0.436230i	−0.008293±0.603532i	−0.006083±0.890767i	−0.003495±1.122754i
	0.5	$\overline{\delta}$ =1/3	−0.009276±0.307706i	−0.008877±0.430639i	−0.008094±0.595924i	−0.005967±0.880324i	−0.003467±1.111554i
		P	−0.009261±0.307567i	−0.008849±0.430291i	−0.008042±0.595002i	−0.005865±0.876955i	−0.003353±1.103705i
10	0	$\overline{\delta}$ =0	**−0.004795±0.221243i**	**−0.004597±0.309687i**	**−0.004222±0.429011i**	**−0.003262±0.638237i**	**−0.002150±0.820656i**
	0.01	$\overline{\delta}$ =1/3	−0.004794±0.221206i	−0.004596±0.309636i	−0.004220±0.428940i	−0.003261±0.638133i	−0.002149±0.820526i
		P	−0.004794±0.221206i	−0.004595±0.309633i	−0.004220±0.428934i	−0.003261±0.638110i	−0.002148±0.820470i
	0.1	$\overline{\delta}$ =1/3	−0.004779±0.220876i	−0.004582±0.309173i	−0.004208±0.428300i	−0.003252±0.637194i	−0.002144±0.819362i
		P	−0.004779±0.220868i	−0.004581±0.309151i	−0.004205±0.428239i	−0.003247±0.636965i	−0.002137±0.818803i
	0.5	$\overline{\delta}$ =1/3	−0.004717±0.219423i	−0.004522±0.307141i	−0.004153±0.425491i	−0.003212±0.633072i	−0.002120±0.814248i
		P	−0.004713±0.219379i	−0.004515±0.307025i	−0.004141±0.425179i	−0.003186±0.631932i	−0.002087±0.811489i

definitions given in Eq. (47), if some root $\overline{\beta}$ is found as $\overline{\beta} = a + \mathrm{i}b$, then, it is observed that $-a-\mathrm{i}b, b+\mathrm{i}a$ and $-b-\mathrm{i}a$ are roots also. In case of "–" sign, $-a+\mathrm{i}b$, $a-\mathrm{i}b, b-\mathrm{i}a$ and $-b+\mathrm{i}a$ also represent roots of the equation. However, fortunately, all of these complex numbers lead at the end, to the same pair of complex conjugate number $\lambda_{1,2}/\omega_0$ which is physically meaningful (i.e., negative real parts).

Various observations can be made from examination of the complex numbers in Table 1 in which $\overline{d} = 0.1, \eta = \alpha_{\overline{M}} = 0.5$ are taken, as stated previously.

The imaginary parts of the "P"-values, i.e., the "exact" non-dimensional "eigenfrequencies" within a $\alpha_M - \alpha_k$ cell get smaller if $\overline{m}_{21}$ gets larger, as expected. Hence, the corresponding values for $\overline{m}_{21} = 0.5$ are always smaller than those for $\overline{m}_{21} = 0.01$. The same trend holds for $\overline{\delta} = 1/3$-values, as well. Table 1 reveals the fact that if α_M gets larger by holding α_k constant, then, the corresponding "eigenfrequencies" get smaller, as expected. On the other hand, it is seen that the corresponding "eigenfrequencies" get larger if α_k gets larger by keeping α_M constant, which can be expected, as the system becomes more stiff.

The absolute values of the relative "errors" of the "eigenfrequencies" in the first sub-cells corresponding to $\overline{m}_{21} = 0$, with respect to the imaginary parts of the "P"-values in each sub-cell of Table 1, which represent "exact" values of the "eigenfrequencies", are shown in Fig. 5 in the form of "error" surfaces, from bottom to top for $\overline{m}_{21} = 0.01$, 0.1 and 0.5, respectively. Where $\eta = 0.5, \overline{d} = 0.1$ and $\alpha_{\overline{M}} = 0.5$ are taken, the relative "errors" surfaces are drawn for various values of the stiffness and mass parameters: α_k and α_M.

It is clearly seen from this figure that the "errors" coming from not taking into account the own mass of the helical spring become more pronounced in the parameter region α_M up to 2 and α_k up to 4. On the other side, the errors decrease if α_M increases, by keeping α_k constant.

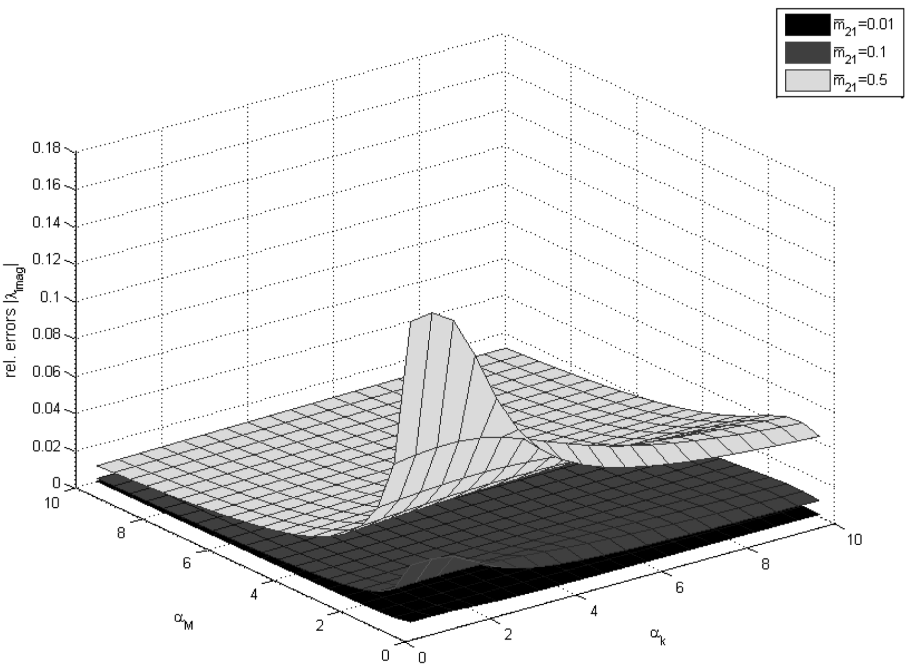

Fig. 5 The relative "errors" of $\overline{m}_{21} = \overline{\delta} = 0$-case with respect to "$P$"-values in each sub-cell of Table 1

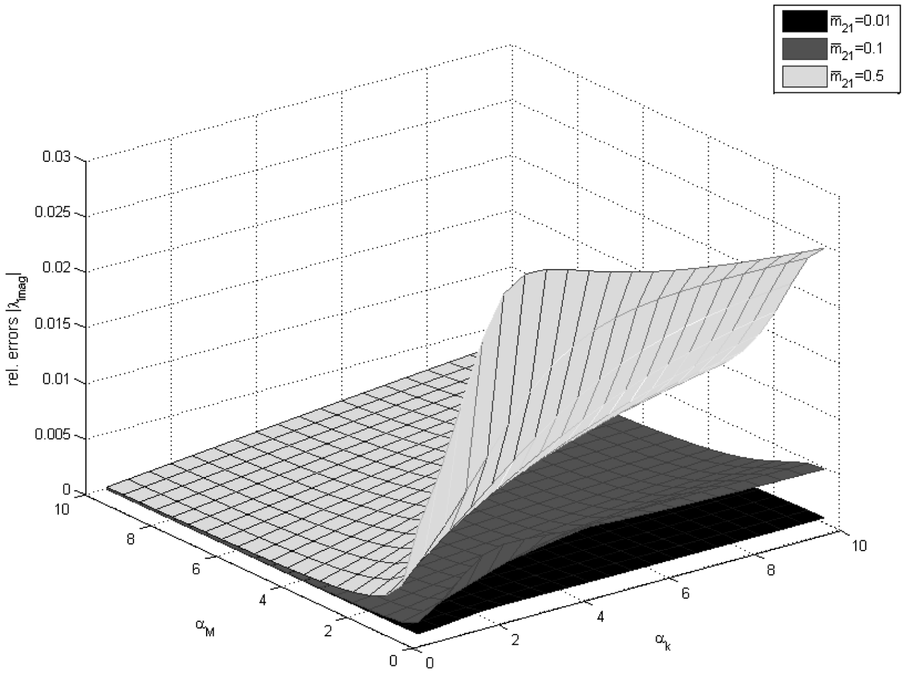

Fig. 6 The relative "errors" of $\overline{\delta}\ =\ 1/3$-case with respect to "*P*"-values in each sub-cell of Table 1

Based on the fact that a design engineer would most probably tend to add one third of the spring mass to the tip mass, it is reasonable also to examine the relative "errors" of the "eigenfrequencies" in case of $\overline{\delta} = 1/3$ with respect to the "exact" values, i.e., "*P*"-values in each sub-cell of Table 1. The corresponding "error" surfaces are shown in Fig. 6, from bottom to top for $\overline{m}_{21} = 0.01$, 0.1 and 0.5, respectively. The relative "error" surfaces are drawn for various combinations of stiffness and mass parameters α_k, and α_M, where $\eta = 0.5, \overline{d} = 0.1$ and $\alpha_{\overline{M}} = 0.5$ are taken. It is clearly seen that the "errors" decrease continuously if α_M increases by keeping α_k fixed. This figure indicates that the errors from applying the $\overline{\delta} = 1/3$ -approach become significant in the parameter region of α_M up to 2. Increasing α_k in this region up to 4 leads to more significant "errors", whereas increasing beyond 4 leads to approximately constant "error" levels. Another fact which should be stated is that these "errors" increase approximately linearly with $\overline{m}_{21}$.

As a second numerical application, the λ/ω_0-values of the system in Fig. 2 are collected in Table 2 for various values of the non-dimensional stiffness parameter α_k where $\overline{m}_{21}$ is taken as 0.01, 0.1 and 0.5. The complex numbers in the second column written in bold represent the eigenvalues of the system in Fig. 2 for the massless spring case, i.e., $\overline{m}_{21} = 0$, hence $\overline{\delta} = 0$. The other system parameters are chosen as: $\overline{d} = 0.1$, $\eta = 0.5$ and $\alpha_{\overline{M}} = 0.5$. The explanations regarding the factor $\overline{\delta}$ are the same as for Table 1, the difference being that now $\overline{\delta} = 1/3$ corresponds to the case where one third of the spring mass is added to the attachment point of the spring-mass to the bending beam, as depicted in Fig. 4.

The first values in each $\alpha_k - \overline{m}_{21}$ cell are obtained from the numerical solutions of characteristic Eq. (A.2) for $\overline{\delta} = 1/3$.

The second complex numbers in the same cell indicated by "*P*" are obtained from the numerical solution of the characteristic Eq. (65), considering the definitions in Eqs. (32) and (47). Finally, it is

Table 2 The characteristic values of the system in Fig. 2 in the form of λ/ω_0, for various values of the stiffness and mass parameter α_k and $\overline{m}_{21}$

			$\overline{m}_{21}$		
α_k	$\overline{\delta}=0$		0.01	0.1	0.5
0.5	−0.006911±2.033428i	$\overline{\delta}=1/3$	−0.006910±2.032960i	−0.006894±2.028755i	−0.006823±2.010287i
		P	−0.006911±2.032957i	−0.006994±2.028521i	−0.011289±2.003208i
1	−0.006860±2.050289i	$\overline{\delta}=1/3$	−0.006858±2.049821i	−0.006843±2.045612i	−0.006774±2.027126i
		P	−0.006858±2.049819i	−0.006869±2.045482i	−0.007648±2.023459i
1.5	−0.006809±2.066889i	$\overline{\delta}=1/3$	−0.006807±2.066420i	−0.006792±2.062209i	−0.006726±2.043707i
		P	−0.006807±2.066419i	−0.006804±2.062120i	−0.007073±2.041316i
2	−0.006758±2.083235i	$\overline{\delta}=1/3$	−0.006757±2.082766i	−0.006743±2.078552i	−0.006678±2.060038i
		P	−0.006757±2.082765i	−0.006749±2.078484i	−0.006862±2.058258i
2.5	−0.006709±2.099334i	$\overline{\delta}=1/3$	−0.006707±2.098864i	−0.006693±2.094650i	−0.006631±2.076126i
		P	−0.006707±2.098864i	−0.006697±2.094595i	−0.006744±2.074702i
3	−0.006659±2.115193i	$\overline{\delta}=1/3$	-0.006658±2.114724i	−0.006644±2.110508i	−0.006584±2.091978i
		P	−0.006658±2.114723i	−0.006647±2.110461i	−0.006661±2.090785i
5	−0.006467±2.176358i	$\overline{\delta}=1/3$	−0.006465±2.175889i	−0.006454±2.171676i	−0.006401±2.153145i
		P	−0.006465±2.175889i	−0.006455±2.171647i	−0.006427±2.152404i
10	−0.006019±2.315258i	$\overline{\delta}=1/3$	−0.006018±2.314793i	−0.006010±2.310621i	−0.005972±2.292236i
		P	−0.006018±2.314793i	−0.006010±2.310604i	−0.005979±2.291827i

worth to noting that these numbers are exactly the same as those obtained from the numerical solution of the characteristic Eq. (59), where the matrix $[\overline{T}_2]$ in the matrix product Eq. (58) is to be taken now as the matrix given in Eq. (67).

The imaginary parts of the "*P*"-values, i.e., the "exact" non-dimensional "eigenfrequencies" relating to constant $\overline{m}_{21}$-values get larger if α_k increases. This can be expected, as the system becomes stiffer, hence, the "eigenfrequencies" will be higher. On the other side, the corresponding "eigenfrequencies" decrease if $\overline{m}_{21}$ increases for a certain α_k-value. It is an expected effect, that increasing masses in a system lead to decreasing "eigenfrequencies".

The absolute values of the relative "errors" of the "eigenfrequencies" in the first-column, corresponding to $\overline{m}_{21} = \overline{\delta} = 0$, with respect to the corresponding "exact eigenfrequencies" in the "*P*"-rows, are shown in Fig. 7 in the form of "error"“-curves for various values of stiffness and mass parameters, α_k and $\overline{m}_{21}$, where $\eta = 0.5, \overline{d} = 0.1$ and $\alpha_{\overline{M}} = 0.5$ are taken. The "error" curves are drawn from bottom to top for $\overline{m}_{21} = 0.01$, 0.1 and 0.5, respectively. It is seen, that the "errors" grow approximately linearly with $\overline{m}_{21}$, which is understandable.

Another fact which can be seen from Fig. 7 is that the "errors" are practically not affected by α_k if $\overline{m}_{21}$ takes relatively small values. However, the $\overline{m}_{21} = 0.5$-curve descends faster in the region of α_k-values up to 2 and then the descend occurs more softly.

Finally, the "errors" of the "eigenfrequencies" arising in case of not considering the own mass of the helical spring, and adding one third of its mass to the attachment point to the horizontal beam, i.e., $\overline{\delta} = 0$ and $\overline{\delta} = 1/3$, with respect to the "exact" values in the "*P*"-rows, are shown in Fig. 8 in the form of "error"-curves,for various values of the stiffness parameter α_k, where $\eta = 0.5, \overline{d} = 0.1$, $\alpha_{\overline{M}} = 0.5$ and $\overline{m}_{21} = 0.5$ are taken. The upper curve corresponds to $\overline{\delta} = 0$, i.e., massless spring

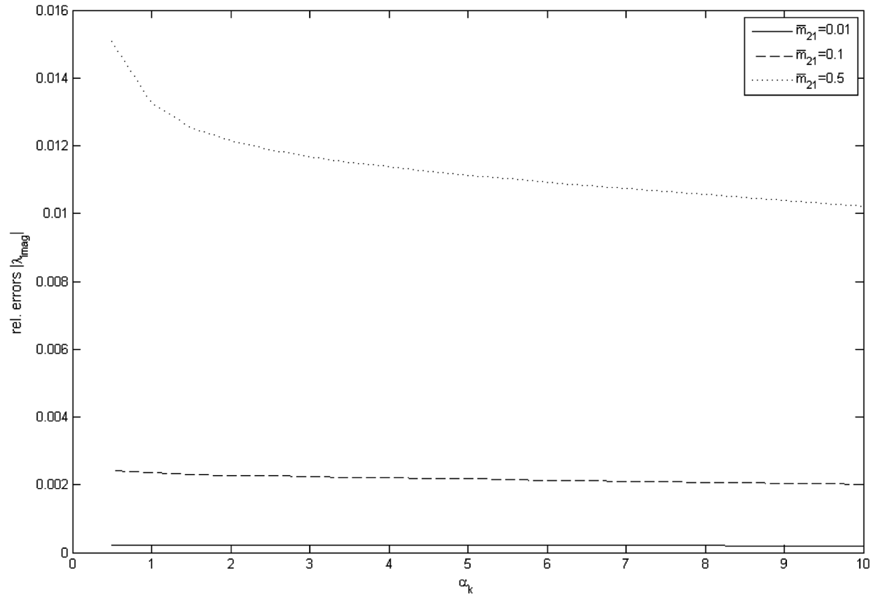

Fig. 7 The relative “errors” of $\overline{m}_{21} = \overline{\delta} = 0$ -case with respect to “*P*”-values in each cell of Table 2

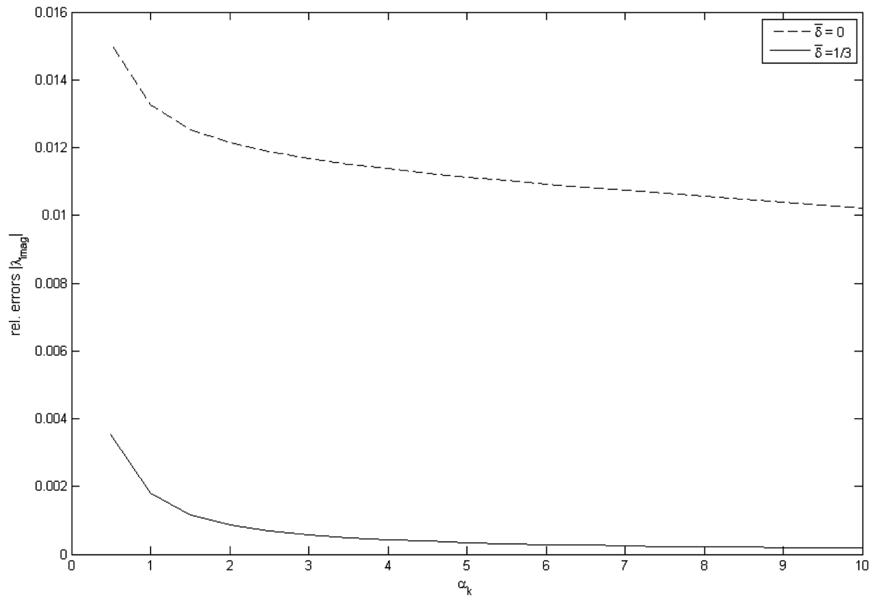

Fig. 8 The relative “errors” of $\overline{\delta} = 0$ and $\overline{\delta} = 1/3$-cases with respect to “*P*”-values in each cell of Table 2

case, whereas the lower curve corresponds to $\overline{\delta} = 1/3$. It can be stated that both curves differ by an approximately constant amount from each other. That the lower curve remains over a wide range of the stiffness parameter beginning approximately with $\alpha_k = 1.5$, less than 0.001 indicates clearly that the $\overline{\delta} = 1/3$ -approach is a quite good approximation which can be applied in a wide range of α_k. On the other side, it is seen that not taking into account the own mass of the helical spring leads to an average error of approximately 1.2 percent in the “eigenfrequencies”, which could be significant for some applications.

4. Conclusions

Many actual vibrational systems encountered in the real life are modeled in the technical literature as Bernoulli-Euler beams subject to various supporting conditions with helical spring-mass attachments. However, in these applications the helical springs are frequently assumed to be massless. The system investigated in the present study consists of a cantilever beam with a tip mass to which a visco-elastic (Kelvin-Voigt model) helical spring-mass is attached in-span. In order to account for the own mass of the helical spring, it is modeled as a longitudinally vibrating visco-elastic rod. The characteristic equation of the combined system above is derived on the basis of two different methods, i.e., via a boundary value problem formulation and the transfer matrix method. Further, the characteristic equation of the reduced system resulting for the tip mass on the rod going to infinity is established as well.

The characteristic equations obtained are then numerically solved for various combinations of the physical parameters. Comparison of the numerical results with the massless spring case and with the engineering approach in which one third of the spring mass would be attached to its end, reveals clearly the fact that both approaches could cause significant errors in the numerical values of especially the complex “eigenfrequencies” of the combined system, for some parameter combinations. Therefore, it is quite reasonable to supply a design engineer working in this area with the “exact” characteristic equations of the systems investigated in the present study in order to enable him to obtain “exact” eigenvalues of these systems.

Acknowledgements

The first author gratefully acknowledges the financial support of Alexander von Humboldt-Foundation for enabling a two month stay at the University of Wuppertal (Germany) in the summer of 2004. He also thanks to his host and friend Professor P. C. Müller for his hospitality and for many fruitful discussions.

References

Cha, P.D. (2001), “Alternative formulations to obtain the eigensolutions of a continuous structure to which spring-mass systems are attached”, *J. Sound Vib.*, **246**, 741-750.

Chen, D.W. and Wu, J.S. (2002), “The exact solutions for the natural frequencies and mode shapes of non-uniform beams with multiple spring-mass systems”, *J. Sound Vib.*, **255**, 299-232.

Gökdağ, H. and Kopmaz, O. (2004), “Eigenfrequencies of a combined system including two continua connected by discrete elements”, *J. Sound Vib.*, **284**, 1203-1216.

Gürgöze, M. (1996a), “On the eigenfrequencies of a cantilever beam with attached tip mass and a spring-mass system”, *J. Sound Vib.*, **190**, 149-162.

Gürgöze, M. (1996b), “On the eigenfrequencies of cantilevered beams carrying a tip mass and spring-mass in-span”, *Int. J. Mech. Sci.*, **38**(12), 1295-1306.

Gürgöze, M. (2005), "On the eigenfrequencies of a cantilever beam carrying a tip spring-mass system with mass of the helical spring considered", *J. Sound Vib.*, **282**, 1221-1230.

Gürgöze, M. and Zeren, S. (2006), "On the eigencharacteristics of an axially vibrating viscoelastic rod carrying a tip mass and its representation by a single degree-of-freedom system", *J. Sound Vib.*, **294**, 388-396.

Gürgöze, M., Çakar, O. and Zeren, S. (2006), "On the frequency equation of a combined system consisting of a simply supported beam and in-span helical spring-mass with mass of the helical spring considered", *J. Sound Vib.*, **295**, 436-449.

James, M.L., Smith, G.M., Wolford, J.C. and Whaley, P.W. (1994) *Vibration of Mechanical and Structural Systems*, HarperCollins College Publishers, New York.

Li, Q.S., Fang, J.Q. and Jeary, A.P. (2000a), "Free vibration analysis of cantilevered tall structures under various axial loads", *Eng. Struct.*, **22**, 525-534.

Li, Q.S., Li, G.Q. and Liu, D.K. (2000b), "Exact solutions for longitudinal vibration of rods coupled by translational springs", *Int. J. Mech. Sci.*, **42**, 1135-1152.

Li, Q.S., Yang, K., Zhang, L. and Zhang, N. (2002), "Frequency domain analysis of fluid–structure interaction in liquid-filled pipe systems by transfer matrix method", *Int. J. Mech. Sci.*, **44**, 2067-2087.

Lord Rayleigh (1945), *Theory of Sound* (two volumes), Dover Publications, New York

Qiao, H., Li, Q.S. and Li, G.O. (2002), "Vibratory characteristics of non-uniform Euler-Bernoulli beams carrying an arbitrary number of spring-mass systems", *Int. J. Mech. Sci.*, **44**, 725-743.

Tauchert, T.R. (1974), *Energy Principles in Structural Mechanics,* McGraw-Hill, New York.

Wu, J.J. (2002), "Alternative approach for free vibration of beams carrying a number of two-degree of freedom spring-mass systems", *J. Struct. Eng.*, **128**, 1604-1616.

Wu, J.J. (2004), "Free vibration analysis of beams carrying a number of two-degree-of-freedom spring-damper-mass systems", *Finite Elem. Anal. Des.,* **40**, 363-381.

Wu, J.J. (2005), "Use of equivalent mass method for free vibration analyses of a beam carrying multiple two-dof spring-mass systems with inertia effect of the helical springs considered", *Int. J. Numer. Meth. Eng.,* **65***,* 653-678.

Wu, J.J. (2006), "Study on the inertia effect of helical spring of the absorber on suppressing the dynamic responses of a beam subjected to a moving load", *J. Sound Vib.,* **297***,* 981-999.

Wu, J.S. and Chou, H.M. (1999), "A new approach for determining the natural frequencies and mode shapes of a uniform beam carrying any number of sprung masses", *J. Sound Vib.,* **220***,* 451-468.

Wu, J.S. and Chen, D.W. (2000), "Dynamic analysis of a uniform cantilever beam carrying a number of elastically mounted point masses with dampers", *J. Sound Vib.,* **229***,* 549-578.

Appendix

$$
\left|\begin{array}{ccccc}
1 & 1 & 1 & 1 & 0 \\
1 & -1 & \mathrm{i} & -\mathrm{i} & 0 \\
e^{\eta\bar{\beta}} & e^{-\eta\bar{\beta}} & e^{\mathrm{i}\eta\bar{\beta}} & e^{-\mathrm{i}\eta\bar{\beta}} & -\mathrm{e}^{\eta\bar{\beta}} \\
e^{\eta\bar{\beta}} & -e^{-\eta\bar{\beta}} & \mathrm{i}e^{\mathrm{i}\eta\bar{\beta}} & -\mathrm{i}e^{-\mathrm{i}\eta\bar{\beta}} & -\mathrm{e}^{\eta\bar{\beta}} \\
e^{\eta\bar{\beta}} & e^{-\eta\bar{\beta}} & -e^{\mathrm{i}\eta\bar{\beta}} & -e^{-\mathrm{i}\eta\bar{\beta}} & -\mathrm{e}^{\eta\bar{\beta}} \\
e^{\eta\bar{\beta}} & -e^{-\eta\bar{\beta}} & -\mathrm{i}e^{\mathrm{i}\eta\bar{\beta}} & \mathrm{i}e^{-\mathrm{i}\eta\bar{\beta}} & -\mathrm{e}^{\eta\bar{\beta}} \\
[\alpha_k \pm \mathrm{i}\bar{d}\bar{\beta}^2]e^{\eta\bar{\beta}} & [\alpha_k \pm \mathrm{i}\bar{d}\bar{\beta}^2]e^{-\eta\bar{\beta}} & [\alpha_k \pm \mathrm{i}\bar{d}\bar{\beta}^2]e^{\mathrm{i}\eta\bar{\beta}} & [\alpha_k \pm \mathrm{i}\bar{d}\bar{\beta}^2]e^{-\mathrm{i}\eta\bar{\beta}} & 0 \\
0 & 0 & 0 & 0 & \mathrm{e}^{\bar{\beta}} \\
0 & 0 & 0 & 0 & (1 + \alpha_{\bar{M}}\bar{\beta})e^{\bar{\beta}}
\end{array}\right.
$$

$$\left.\begin{array}{cccc}
0 & 0 & 0 & 0 \\
0 & 0 & 0 & 0 \\
-e^{-\eta\bar{\beta}} & -e^{\mathrm{i}\eta\bar{\beta}} & -e^{-\mathrm{i}\eta\bar{\beta}} & 0 \\
e^{-\eta\bar{\beta}} & -\mathrm{i}e^{\mathrm{i}\eta\bar{\beta}} & \mathrm{i}e^{-\mathrm{i}\eta\bar{\beta}} & 0 \\
-e^{-\eta\bar{\beta}} & e^{\mathrm{i}\eta\bar{\beta}} & e^{-\mathrm{i}\eta\bar{\beta}} & 0 \\
e^{-\eta\bar{\beta}} & \mathrm{i}e^{\mathrm{i}\eta\bar{\beta}} & -\mathrm{i}e^{-\mathrm{i}\eta\bar{\beta}} & (\alpha_M + \bar{\delta}\bar{m}_{21})\bar{\beta} \\
0 & 0 & 0 & [(\alpha_M + \bar{\delta}\bar{m}_{21})\bar{\beta}^4 \mp \mathrm{i}\bar{d}\bar{\beta}^2 - \alpha_k] \\
e^{-\bar{\beta}} & -e^{\mathrm{i}\bar{\beta}} & -e^{-\mathrm{i}\bar{\beta}} & 0 \\
-(1-\alpha_{\bar{M}}\bar{\beta})\mathrm{e}^{-\bar{\beta}} & -(\mathrm{i}-\alpha_{\bar{M}}\bar{\beta})\mathrm{e}^{\mathrm{i}\bar{\beta}} & (\mathrm{i}+\alpha_{\bar{M}}\bar{\beta})\mathrm{e}^{-\mathrm{i}\bar{\beta}} & 0
\end{array}\right| = 0 \qquad \text{(A1)}$$

$$\left|\begin{array}{ccccc}
1 & 1 & 1 & 1 & 0 \\
1 & -1 & \mathrm{i} & -\mathrm{i} & 0 \\
e^{\eta\bar{\beta}} & e^{-\eta\bar{\beta}} & e^{\mathrm{i}\eta\bar{\beta}} & e^{-\mathrm{i}\eta\bar{\beta}} & -e^{\eta\bar{\beta}} \\
e^{\eta\bar{\beta}} & -e^{-\eta\bar{\beta}} & \mathrm{i}e^{\mathrm{i}\eta\bar{\beta}} & -\mathrm{i}e^{-\mathrm{i}\eta\bar{\beta}} & -e^{\eta\bar{\beta}} \\
e^{\eta\bar{\beta}} & e^{-\eta\bar{\beta}} & -e^{\mathrm{i}\eta\bar{\beta}} & -e^{-\mathrm{i}\eta\bar{\beta}} & -e^{\eta\bar{\beta}} \\
(1-\psi)e^{\eta\bar{\beta}} & -(1+\psi)e^{-\eta\bar{\beta}} & -(\mathrm{i}+\psi)e^{\mathrm{i}\eta\bar{\beta}} & (\mathrm{i}-\psi)e^{-\mathrm{i}\eta\bar{\beta}} & -e^{\eta\bar{\beta}} \\
0 & 0 & 0 & 0 & e^{\bar{\beta}} \\
0 & 0 & 0 & 0 & (1+\alpha_{\bar{M}}\bar{\beta})\mathrm{e}^{\bar{\beta}}
\end{array}\right.$$

$$\left.\begin{array}{ccc}
0 & 0 & 0 \\
0 & 0 & 0 \\
-e^{-\eta\bar{\beta}} & -e^{\mathrm{i}\eta\bar{\beta}} & -e^{-\mathrm{i}\eta\bar{\beta}} \\
e^{-\eta\bar{\beta}} & -\mathrm{i}e^{\mathrm{i}\eta\bar{\beta}} & \mathrm{i}e^{-\mathrm{i}\eta\bar{\beta}} \\
-e^{-\eta\bar{\beta}} & e^{\mathrm{i}\eta\bar{\beta}} & e^{-\mathrm{i}\eta\bar{\beta}} \\
e^{-\eta\bar{\beta}} & \mathrm{i}e^{\mathrm{i}\eta\bar{\beta}} & -\mathrm{i}e^{-\mathrm{i}\eta\bar{\beta}} \\
e^{-\bar{\beta}} & -e^{\mathrm{i}\bar{\beta}} & -e^{-\mathrm{i}\bar{\beta}} \\
-(1-\alpha_{\bar{M}}\bar{\beta})\mathrm{e}^{-\bar{\beta}} & -(\mathrm{i}-\alpha_{\bar{M}}\bar{\beta})\mathrm{e}^{\mathrm{i}\bar{\beta}} & (\mathrm{i}+\alpha_{\bar{M}}\bar{\beta})\mathrm{e}^{-\mathrm{i}\bar{\beta}}
\end{array}\right| = 0 \qquad \text{(A2)}$$

with

$$\psi := \frac{\alpha_k}{\bar{\beta}^3} \pm i\frac{\bar{d}}{\bar{\beta}} - \bar{\delta}\bar{m}_{21}\bar{\beta}$$